

Microstructure and fractal characteristics of the solid-liquid interface forming during directional solidification of Inconel 718

*WANG Ling^{1,2}, DONG Jian-xin¹, LIU Lin³ and ZHANG Mai-cang¹

(1. High Temperature Materials Research Laboratories, University of Science and Technology Beijing, Beijing 100083, China; 2. School of Materials, Hebei University of Science and Technology, Shijiazhuang 050054, China; 3. National Key Laboratory of Solidification Technology, Northwestern Polytechnical University, Xi'an 710072, China)

Abstract: The solidification microstructure and fractal characteristics of the solid-liquid interfaces of Inconel 718, under different cooling rates during directional solidification, were investigated by using SEM. Results showed that 5 $\mu\text{m/s}$ was the cellular-dendrite transient rate. The prime dendrite arm spacing (PDAS) was measured by Image Tool and it decreased with the cooling rate increased. The fractal dimension of the interfaces was calculated and it changes from 1.204310 to 1.517265 with the withdrawal rate ranging from 10 to 100 $\mu\text{m/s}$. The physical significance of the fractal dimension was analyzed by using fractal theory. It was found that the fractal dimension of the dendrites can be used to describe the solidification microstructure and parameters at low cooling rate, but both the fractal dimension and the dendrite arm spacing are needed in order to integrally describe the evaluation of the solidification microstructure completely.

Key words: Inconel 718; cooling rate; microstructure; fractal dimension; solid-liquid interface

CLC number: TG132.3*2

Document Code: A

Article ID: 1672-6421(2007)03-182-04

Inconel 718 is a Ni-Cr-Fe based superalloy designed by International Nickel Corporation. Its main alloying elements are Nb, Mo, Ti and Al. The alloy is strengthened by precipitation of A_3B type face center structured γ' and body centered tetragonal γ'' . Because of its excellent properties at medium temperature, Inconel 718 alloy finds extensive application in aerospace industry, nuclear power plant and petrochemical industry as well. It was recognized as a universal alloy. But there are few researches on the solidification of Inconel 718 because the solidification of the alloy is a very complex process. Recently, computational simulation of solidification has been developed quickly [1-4] and fractal theory has provided a powerful tool for quantitative investigation of the solid-liquid interface morphology, and these kinds of evolution are always important subjects in solidification science [5]. It has been developed and applied successfully in many fields in material science, such as the investigations of metal fracture, phase transformation of alloys [6-8]. In this paper the microstructure, PDAS and the fractal dimension of solid-liquid interface of Inconel 718 alloy, under different cooling rates during directional solidification, were

investigated to provide some useful data for the study of solidification of Inconel 718.

1 Experimental procedures

The composition of Inconel 718 alloy used in this study was listed in Table 1. The alloy under study was directionally solidified in a vacuum induction furnace and quenched in liquid metal (LMQ). Each sample [7 mm in diameter \times (90–100) mm in length] was contained in an alumina tube which was withdrawn at the rates ranging from 2 to 100 $\mu\text{m/s}$. The designed withdrawal rates were 2 $\mu\text{m/s}$, 5 $\mu\text{m/s}$, 10 $\mu\text{m/s}$, 20 $\mu\text{m/s}$, 40 $\mu\text{m/s}$, 70 $\mu\text{m/s}$ and 100 $\mu\text{m/s}$, respectively. The thermal gradient was about 10 $^\circ\text{C/mm}$ at the solidification front. The samples were quenched into liquid metal before complete solidification to reserve the microstructure at the solid-liquid interface.

Table 1 Chemical composition of Inconel 718

Al	Mo	Fe	Cr	Nb	Ti	C	Ni
0.56	2.98	19.93	17.72	5.36	0.97	0.021	Bal.

All the SEM samples were ground by 1000-grit sand paper and mechanically polished, and then they were electro etched by connecting to the anode in a solution of CrO_3 , H_2SO_4 and H_3PO_4 at a voltage of 10 V for 10 seconds. The microstructure of these etched samples was studied by using a S250 scanning electron microscope. The solidification microstructure and the

*WANG Ling

Female, born in 1970, Ph.D. A researcher of high temperature materials.

E-mail: sjzhwl@126.com

Received: 2006-07-22; Accepted: 2007-05-31

fractal dimensions under different withdrawal rates were analyzed by means of SEM and Image Tool.

2 Results

2.1 Microstructure of the solid-liquid interface at different cooling rates

The solid-liquid interfaces at cooling rates of 2 $\mu\text{m/s}$ and 5 $\mu\text{m/s}$

were shown in Fig. 1. It was typical cellular structure at cooling rate of 2 $\mu\text{m/s}$, as shown in Fig. 1 (a). The cooling rate of 5 $\mu\text{m/s}$ was the critical rate for cellular-dendrite transition and the solid-liquid interface under 5 $\mu\text{m/s}$ was cellular-dendrite mixed structure as shown in Fig.1 (b). There were both cellular grains and dendrites in the interface. It can be seen from Fig. 1 (c) that there were small secondary dendrites forming in the primary one, but the secondary dendrites were very small and not well developed.

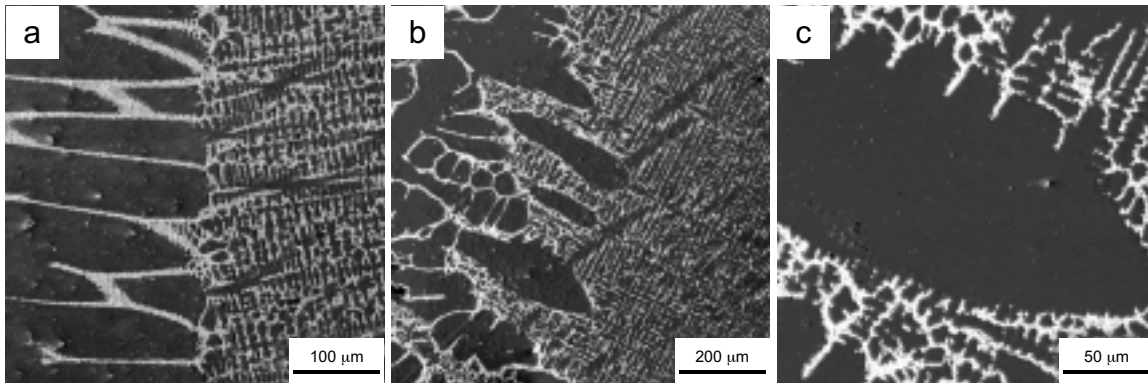


Fig. 1 The solid-liquid interfaces at cooling rates of (a) 2 $\mu\text{m/s}$, (b) 5 $\mu\text{m/s}$ and (c) 5 $\mu\text{m/s}$

When the cooling rates were higher than 5 $\mu\text{m/s}$, the solid-liquid interfaces were typical dendrites. The dendrite solid-liquid interfaces at cooling rate ranging from 10 $\mu\text{m/s}$ to 100 $\mu\text{m/s}$ were shown in Fig. 2. The dendrites become remarkably finer as the

cooling rate increased from 10 $\mu\text{m/s}$ to 100 $\mu\text{m/s}$. The secondary dendrites become more and more and the dendrites become finer and finer. The interface becomes more indistinguishable under higher cooling rate as well.

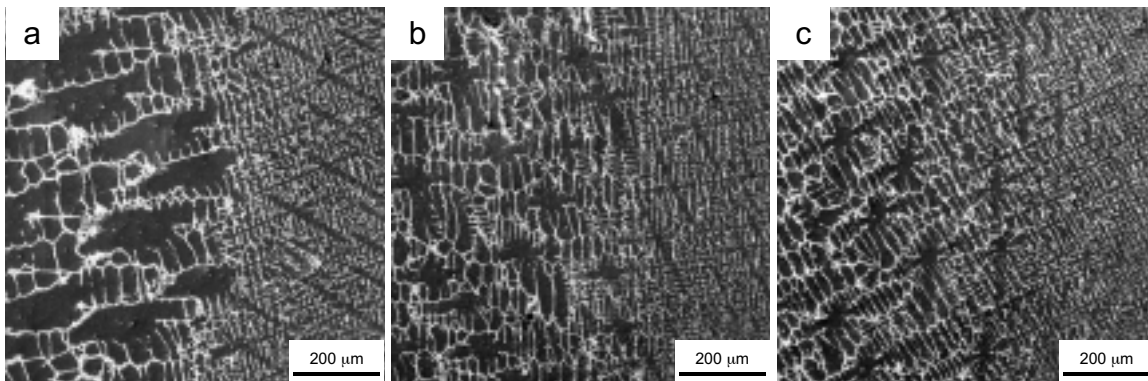


Fig. 2 Dendrite solid-liquid interfaces at cooling rates of (a) 10 $\mu\text{m/s}$; (b) 40 $\mu\text{m/s}$ and (c) 100 $\mu\text{m/s}$

2.2 Primary dendrite arm spacing at different cooling rates

The primary dendrite arm spacing at different cooling rates were measured. Figure 3 gives the variation of primary dendrite arm spacing (PDAS) vs. cooling rates. PDAS decreased remarkably with increasing of the cooling rate in the range of 10–40 $\mu\text{m/s}$, but the decreasing rate became slower when the cooling rate was higher than 40 $\mu\text{m/s}$.

2.3 Fractal characteristic of the solid-liquid interface

The fractal dimensions under different withdrawal rates were analyzed by means of SEM and Image Tool according to equation $N=Fr^{-D}$, where N is the square lattice number which covers the

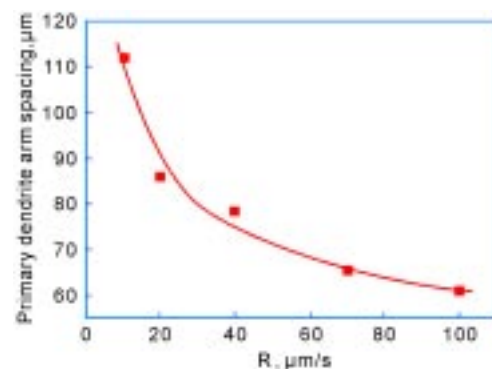


Fig. 3 Primary dendrite arm spacing under different cooling rates

surface border, F is a constant, D the fractal dimension and r the dimension size in measurement. The smaller the r , the more accurate the surface structure. D represents the corresponding fractal dimension when setting r approaches to zero. The fractal dimensions at cooling rates of $2 \mu\text{m/s}$ and $20 \mu\text{m/s}$ were shown in Fig. 4. The slop of each line is the fractal dimension at that particular rate. The fractal dimensions at $2 \mu\text{m/s}$ and $20 \mu\text{m/s}$ were 1.029950 and 1.360185, respectively. All the fractal dimensions at cooling rates from $10 \mu\text{m/s}$ to $100 \mu\text{m/s}$ were shown in Fig. 5. It can be seen that the fractal dimension increased quickly with the cooling rates increased, but the increasing rate slow down gradually when the cooling rate was higher than $40 \mu\text{m/s}$.

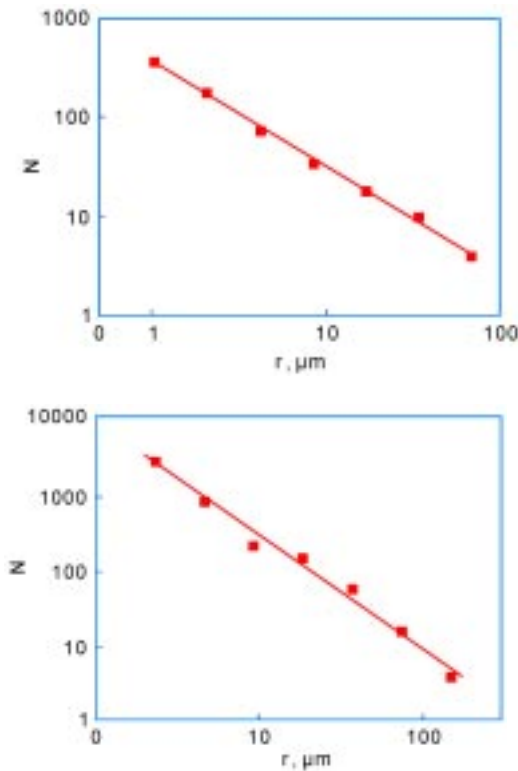


Fig. 4 Relationship between N and r at cooling rates of (a) $R=2 \mu\text{m/s}$ ($D=1.02995$) and (b) $R=20 \mu\text{m/s}$ ($D=1.360185$).

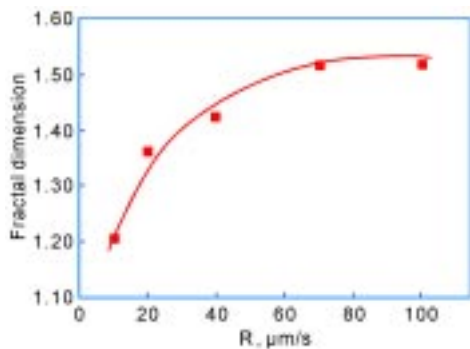


Fig. 5 Fractal dimension at different cooling rates

3 Discussions

Usually, alloy solidification process, such as casting, is carried out in an open system; it exchanges energy and mass with the

environment continuously. During solidification of Inconel 718 alloy, the effect of cooling rate on the interaction in the system and the energy exchange can be shown in two ways: one is by changing the morphology of a single state; the other is the whole numbers (such as more dendrites). The variation of fractal dimension shows the former, while the dendrite arm spacing reflects the latter [5].

During the dendrite growth at lower cooling rates, most energy was consumed in forming the complicated morphology and the fractal dimension increases quickly with the increase of cooling rate. As a kind of fractal structure, the solid-liquid interface has the physical mechanism of the non-linear, random and dissipation of the systems [5, 7, 8]. It is a dissipative structure system in the thin layer (with a thickness of several atoms), which located at the solidification front. Based on self-organization theory, a dissipative structure depends on the production of super-entropy in an open system:

$$\frac{d}{dt} \left(\frac{1}{2} \delta^2 s \right) = -\frac{1}{T} \int dV \left[\sum_i \delta J_i \delta \left(\nabla \frac{\mu_i}{T} \right) + \sum \delta U_p \delta \left(\frac{\varphi}{T} \right) \right]$$

Where J_i is the diffusion flux, $\nabla \frac{\mu_i}{T}$ the chemical potential gradient along the temperature (T) distribution, U_p the rate of chemical reaction, $\frac{\varphi}{T}$ the chemical force and $\frac{d}{dt} \left(\frac{1}{2} \delta^2 s \right)$ the negative entropy flow, i.e. the producing of the super-entropy. There is only very little carbide of MC type forming in the freezing range and it can be assumed that there is no chemical reaction during Inconel 718 solidification. The increase of the cooling rate leads to the increase of both δJ_i and $\delta \left(\nabla \frac{\mu_i}{T} \right)$, which makes the negative entropy flow increasing, so that the entropy becomes smaller and smaller. Set S as entropy and set δ as the measuring size, then according to the definition of the fractal dimension:

$$D \approx -S(\delta)$$

Thus the higher the cooling rates, the higher the fractal dimensions.

A large fractal dimension indicates more intensive non-linear interaction. In directional solidification, the atom concentration at the solidification front becomes higher with the increase of the cooling rate and the interactions between atoms are more intensive. Furthermore, the increase in undercooling results in larger atomic clusters to transform synergistically into non-equilibrium structures within a short time, which requires more intensive interactions and makes the fractal dimension increase with the increase of the cooling rates. On the other hand, the fractal dimension exhibits the extent of the energy exchange between the system and the environment, i.e. dissipation. As shown in Figs. 2 and 6, the higher the cooling rate, the more the energy consumed, the more complicated the morphology of the solid-liquid interface and the higher the fractal dimension. Figure 6 (b) and (d) showed that the solid-liquid interface at $10 \mu\text{m/s}$ was straighter and smoother than that of $40 \mu\text{m/s}$.

The increase in fractal dimension with increase in cooling rates was non-linear. The increasing rate slowed down at higher cooling rates because some of the energy provided by cooling was consumed in increasing the number at higher cooling rate.

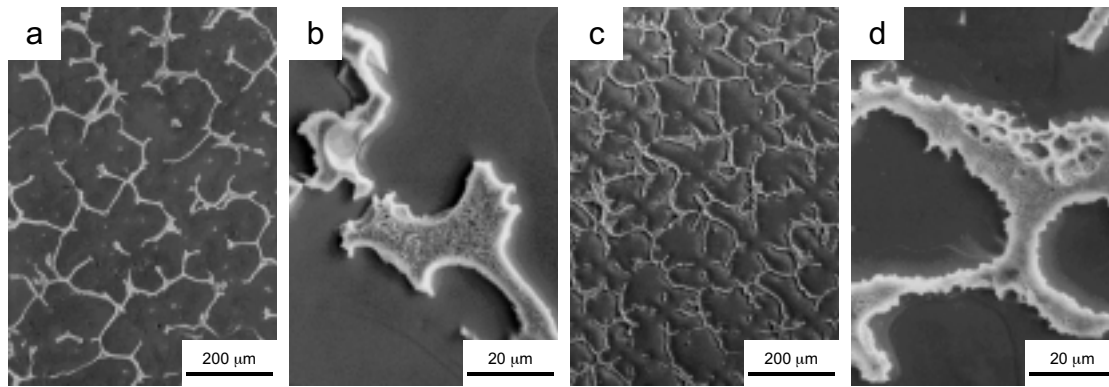


Fig. 6 Cross- sections under different cooling rates: (a) and (b) 10 $\mu\text{m/s}$; (c) and (d) 40 $\mu\text{m/s}$.

It can be seen from Fig. 2 and Fig. 6 (a) and (c) that there were more fine dendrites at higher cooling rate, also the dendrite arm spacing became smaller and the grains were being refined as the cooling rates changed from 10 $\mu\text{m/s}$ to 100 $\mu\text{m/s}$ (Fig. 3). The variation of PDAS with cooling rate increase agrees with that the PDAS is in proportion to the value of $(R \cdot G)^{-\alpha}$, where α is a constant less than 1 and varies with different conditions, and R and G are crystal growth rate and thermal gradient, respectively^[9].

Therefore, the fractal dimension in solidification reflects the extent of complication for the pattern and can describe the morphological feature to some extent. In general, it can be used partially to describe the solidification process. To describe the evaluation of the solidification structure completely and integrally, both the fractal dimension and the dendrite arm spacing or cellular arm spacing have to be considered. Only when the dendrite have grown sufficiently well or the cellular grains have stable morphology, the fractal dimension and the dendrite arm spacing represent the solidification feature.

4 Conclusions

The solidification microstructure and fractal dimension of the solid-liquid interface of Inconel 718 alloy were investigated at different cooling rates. The cooling rate of 5 $\mu\text{m/s}$ was the cellular-dendrite transient rate. The primary dendrite arm spacing decreased with cooling rate increased. The fractal dimension of dendrite was apparently affected by the solidification rate and it increased with a higher rate, but the increment becomes less at higher cooling rate. The fractal dimension exhibits non-linearity and dissipation of energy and mass in solidification by changing the morphology of the structure. Therefore, the concept of fractal can be used to describe the solidification structure only when

most of the energy was consumed in the change in morphology, such as dendrite growth at low cooling rate. In general, both the fractal dimension and the dendrite arm spacing or cellular arm spacing need to be considered in order to describe the evaluation of the solidification microstructure completely and integrally.

References

- [1] Sanyal D, Ramachandrarao P, Gupta O P. A fractal description of transport phenomena in dendritic porous network. *Chemical Engineering Science*, 2006, 61: 307–315.
- [2] GUO Hong-min, YANG Xiang-jie. Multi-scale modeling of solidification microstructure. *The Chinese Journal of Nonferrous Metals*, 2004(1): 928–933. (in Chinese)
- [3] Williamson A. Saigal A. Applications of self-defined arrays for pattern-forming alloy solidification. *Computational Materials Science*, 1998, 11: 27–34.
- [4] Shibkov AA, Golovin Y I, Zheltov MA, *et al.* Morphology diagram of nonequilibrium patterns of ice crystals growing in supercooled water. *Physica A*, 2003, 319: 65–79.
- [5] YANG Ai-min, XIONG Yu-hua, LIU Lin. Fractal characteristics of dendrite and cellular structure in nickel-based superalloy at intermediate cooling rate. *Science and Technology of Advanced Materials*, 2001(2): 101–103.
- [6] QU Zhao-xia, ZHANG Han-qian. Progress of application of fractal theory to material science. *Aerospace Materials Technology*, 1995 (5): 5–9. (in Chinese)
- [7] SUN Li-ling, DONG Lian-ke, ZHANG Jing-hua. The application of fractal theory in the investigation of the solid-liquid interface during solidification. *Material engineering*, 1994 (4): 24–26. (in Chinese)
- [8] SUN Li-ling, DONG Lian-ke, ZHANG Jing-hua. Fractal description of grain boundary configuration in directionally solidified superalloys. *Acta Metallurgica Sinica*. 1994(5), 30 A: 200–203. (in Chinese)
- [9] ZHOU Yao-he, HU Zhuang-qi, JIE Wan-qi. Solidification Technology. Beijing: *China Machine Press*, 1998. (in Chinese)

This work was financially supported by the National Natural Science Foundation of China (No. 50371006).